Electronic Supplementary Information

Novel Pd(II) pincer complexes bearing salicylaldimine−based benzothiazole derivatives: synthesis, structural characterization, DNA/BSA binding, and biological evaluation

Sutthida Wongsuwan,[a] Jaruwan Chatwichien,[b,c] Weekit Sirisaksoontorn,[a] Kittipong Chainok,[d] Apisit Songsasen*[a] and Ratanon Chotima*[e]

[a]Department of Chemistry, Faculty of Science, Kasetsart University, 10900 Bangkok, Thailand

[b]Program in Chemical Sciences, Chulabhorn Graduate Institute, Chulabhorn Royal Academy, 10210 Bangkok, Thailand

[c]Center of Excellence on Environmental Health and Toxicology (EHT), OPS, MHESI, Thailand

[d]Thammasat University Research Unit in Multifunctional Crystalline Materials and Applications (TU−MCMA), Faculty of Science and Technology, Thammasat University, 12121 Pathum Thani, Thailand

[e]Department of Chemistry, Faculty of Science, Naresuan University, 65000 Phitsanulok, Thailand.

Corresponding authors:

E−mail: R.C. (ratanonc@nu.ac.th) and A.S. (fsciass@ku.ac.th)

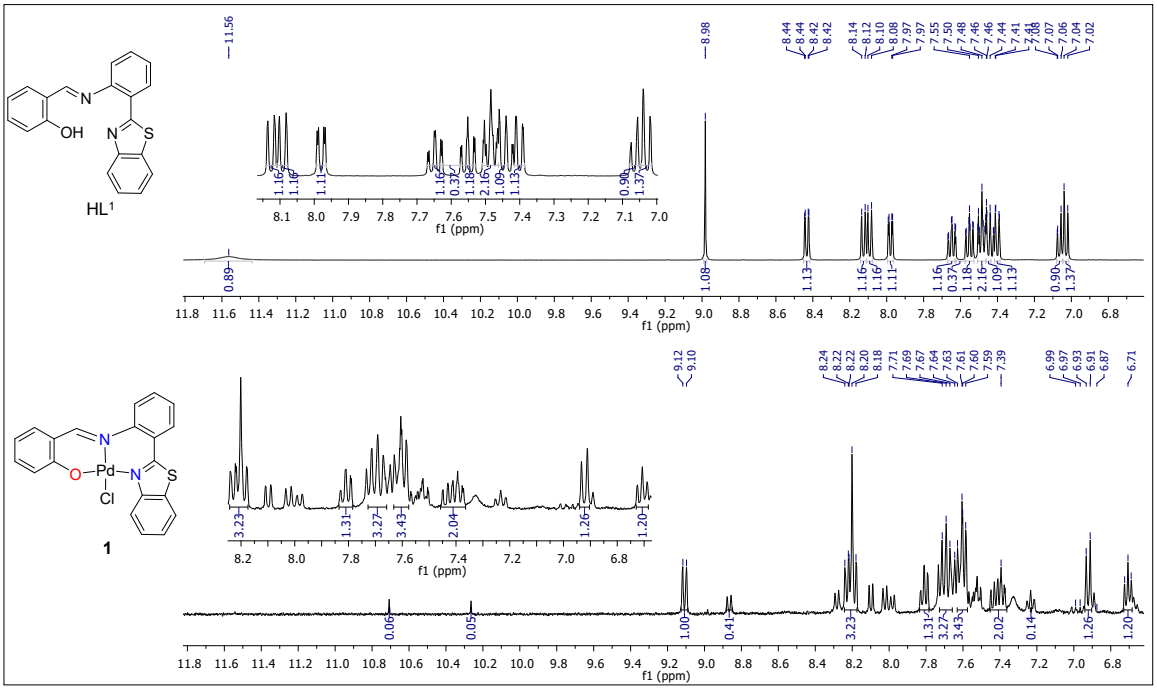

Fig. S1 ^{1}H NMR (400 MHz, DMSO−d_6) spectra of ligand HL^{1} and Pd(II) complex **1**.

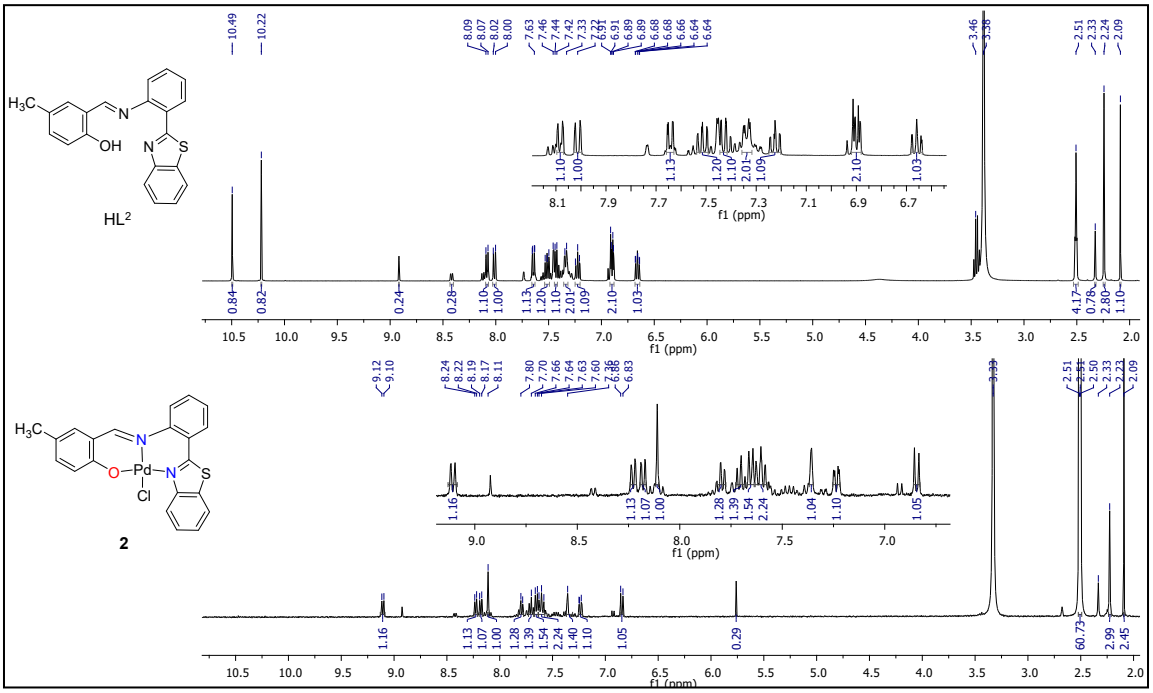

Fig. S2 ^{1}H NMR (400 MHz, DMSO−d_6) spectra of ligand HL^{2} and Pd(II) complex **2**.

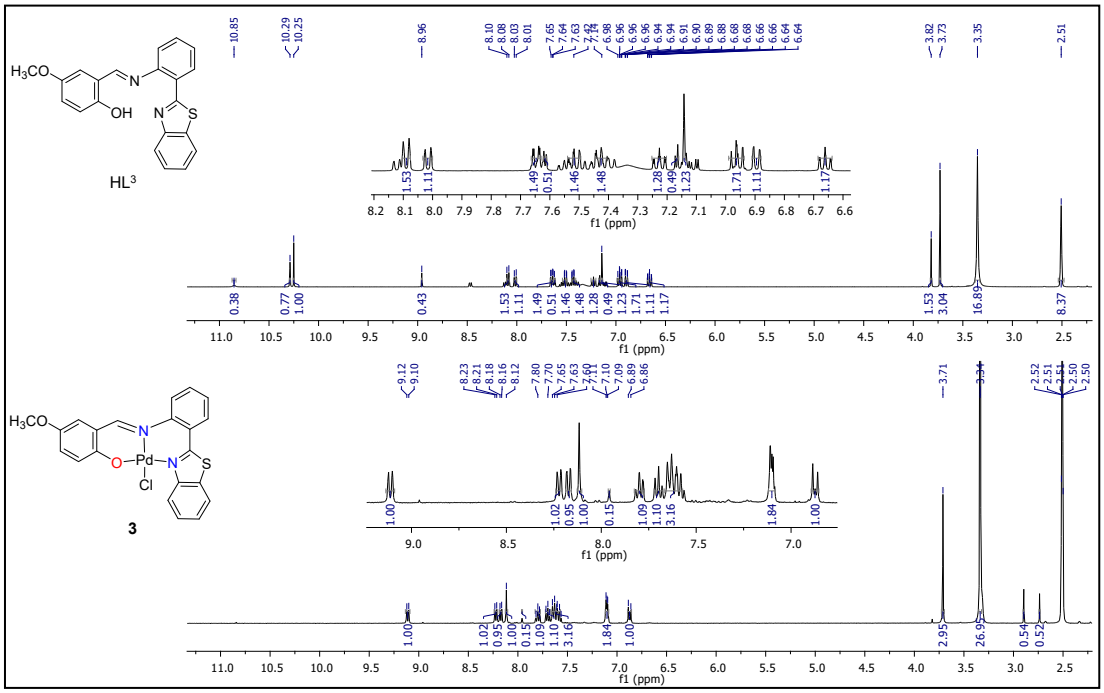

Fig. S3 ^{1}H NMR (400 MHz, DMSO−d_6) spectra of ligand HL^3 and their Pd(II) complex **3**.

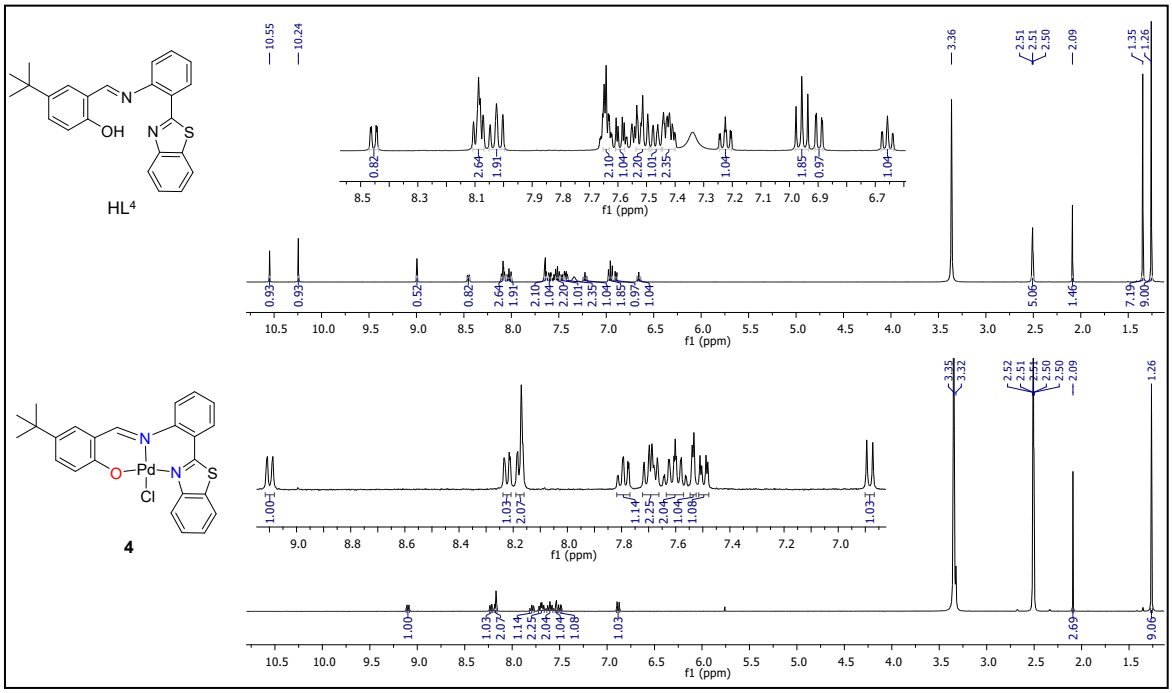

Fig. S4 ^{1}H NMR (400 MHz, DMSO−d_6) spectra of ligand HL^4 and Pd(II) complex **4**.

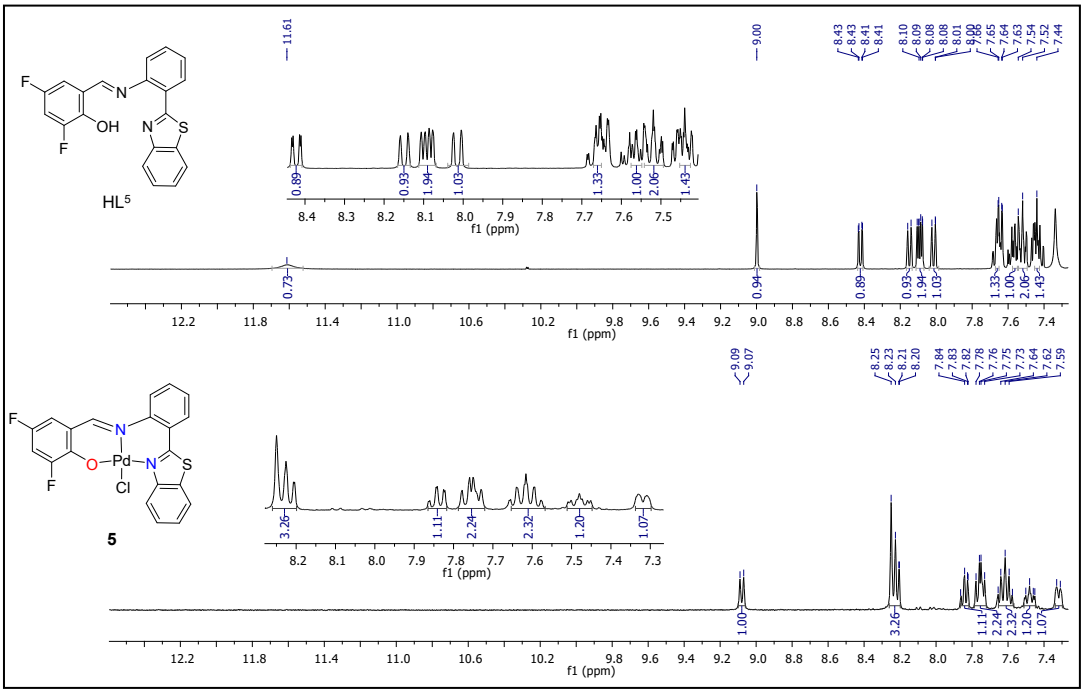

Fig. S5 ^{1}H NMR (400 MHz, DMSO−d_6) spectra of ligand HL^5 and Pd(II) complex **5**.

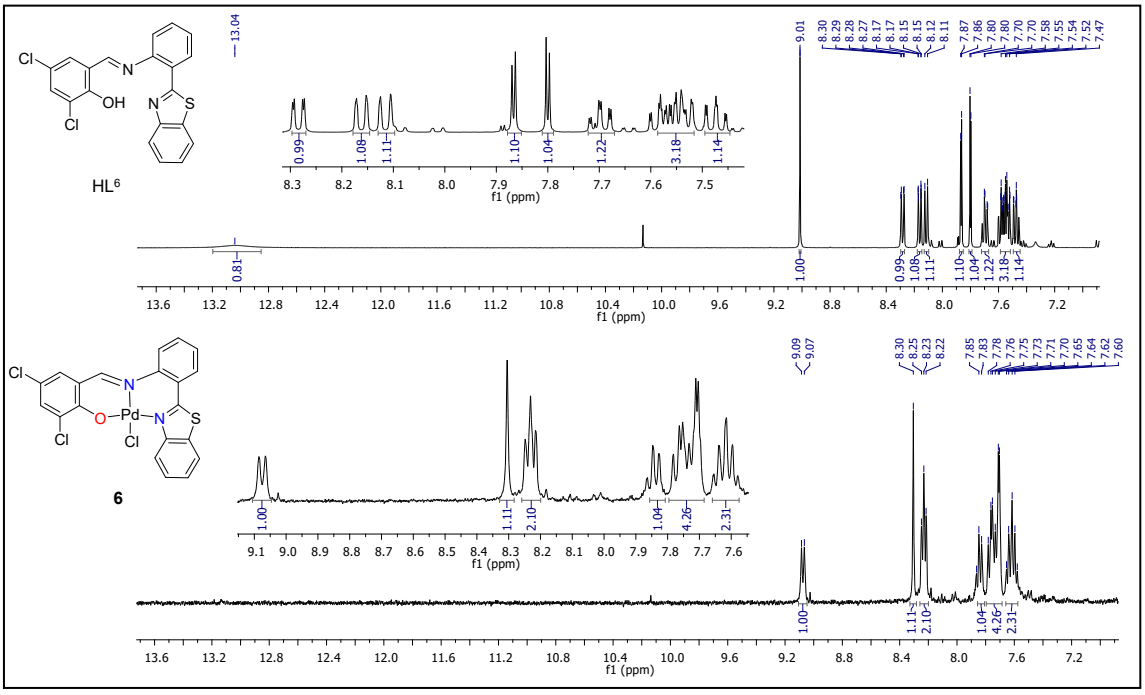

Fig. S6 ^{1}H NMR (400 MHz, DMSO−d_6) spectra of ligand HL^6 and Pd(II) complex **6**.

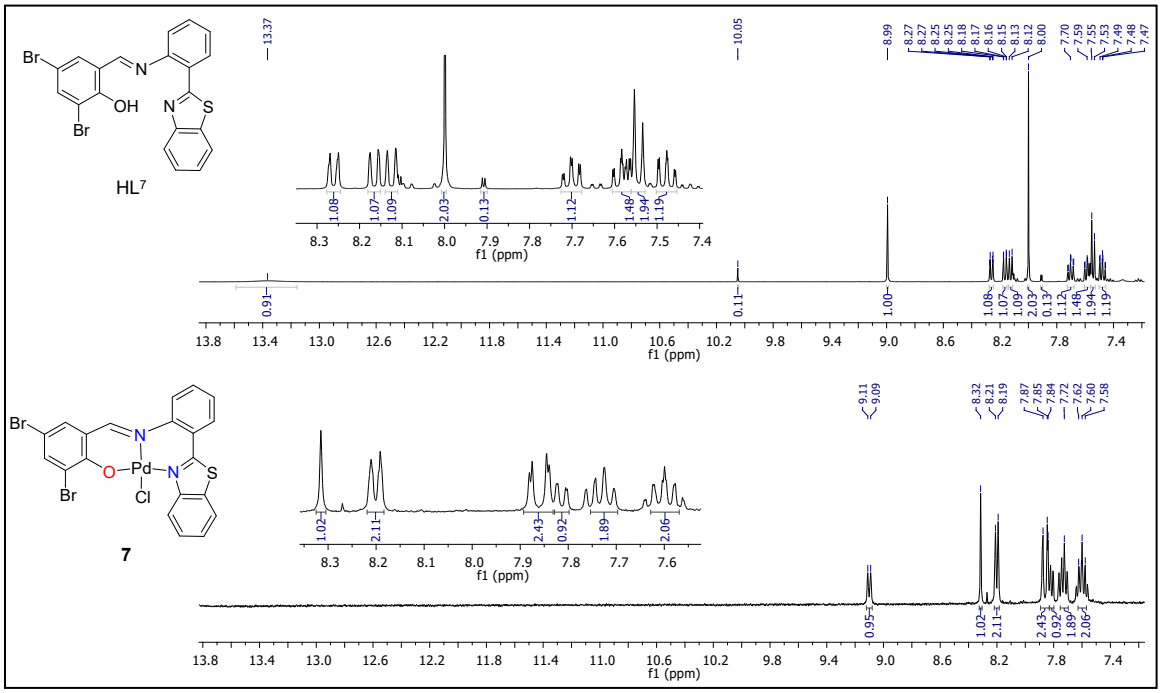

Fig. S7 ^{1}H NMR (400 MHz, DMSO−d_6) spectra of ligand HL^7 and Pd(II) complex **7**.

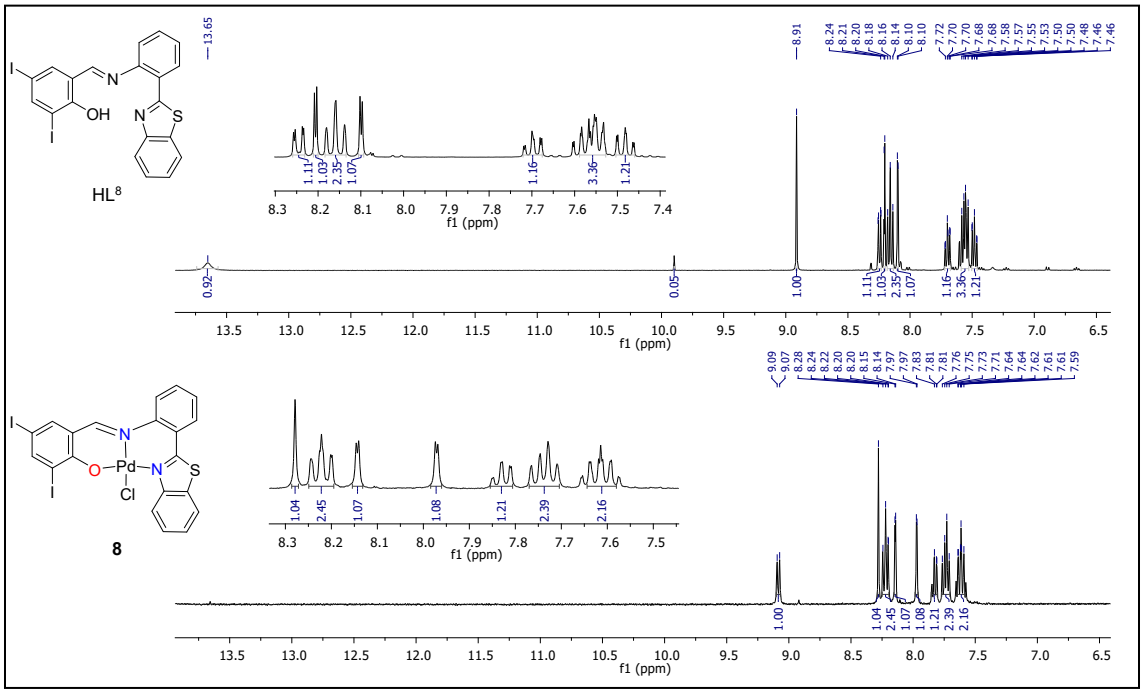

Fig. S8 ^{1}H NMR (400 MHz, DMSO−d_6) spectra of ligand HL^8 and Pd(II) complex **8**.

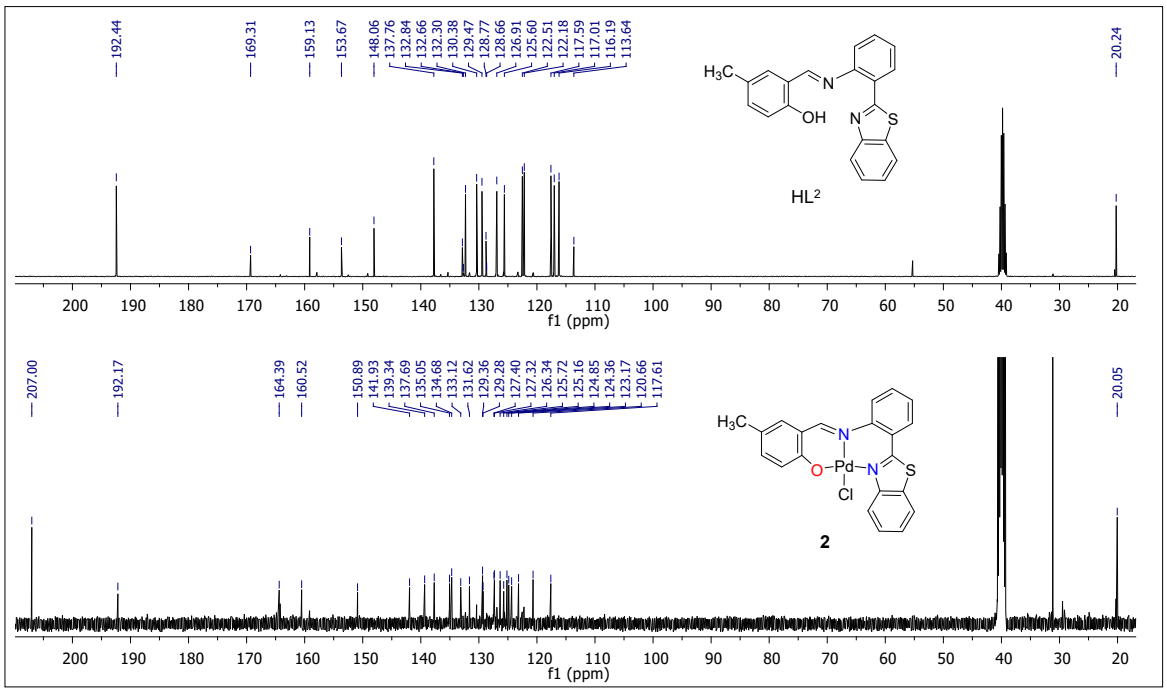

Fig. S9 ^{13}C NMR (100 MHz, DMSO−d_6) spectra of ligand HL^2 and Pd(II) complex **2**.

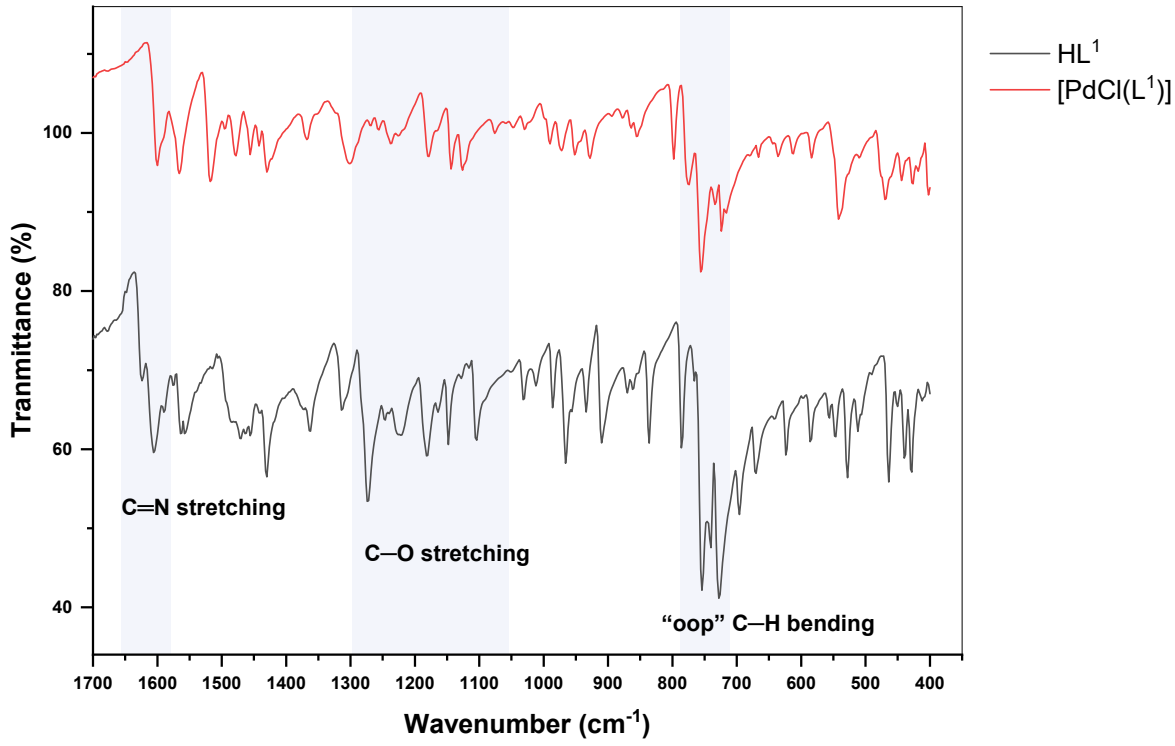

Fig. S10 FT-IR (ATR) spectra of ligand HL^1 and Pd(II) complex **1**.

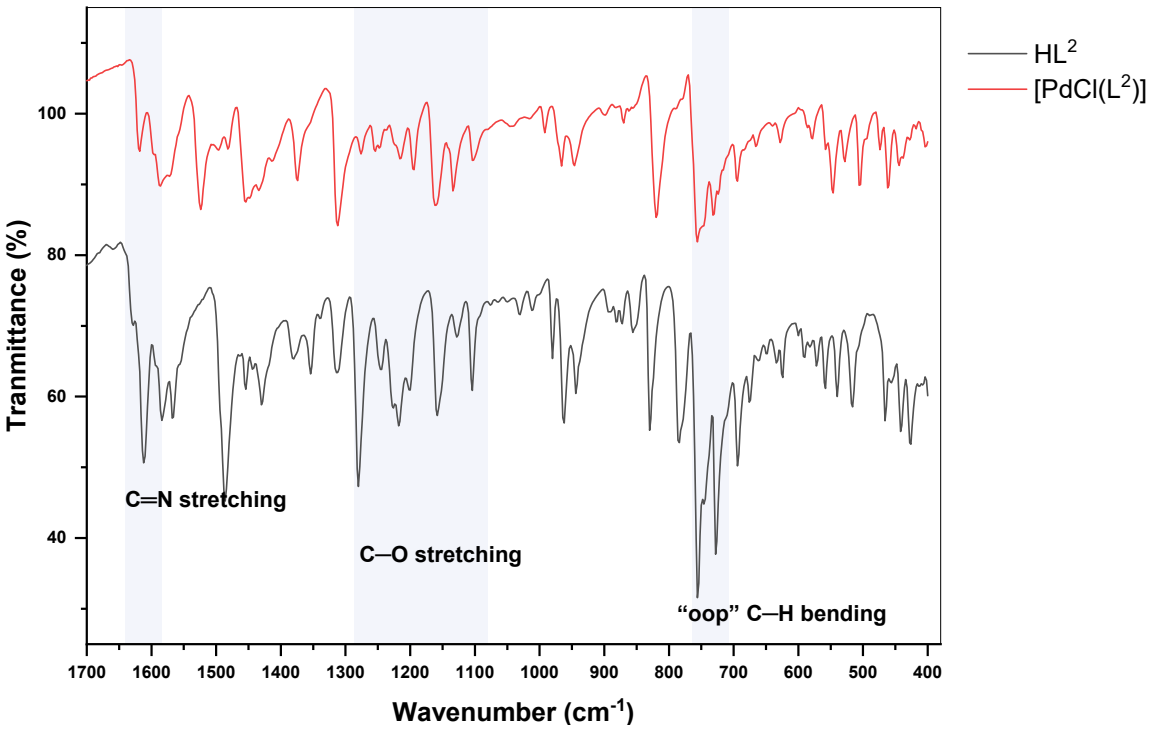

Fig. S11 FT-IR (ATR) spectra of ligand HL^2 and Pd(II) complex **2**.

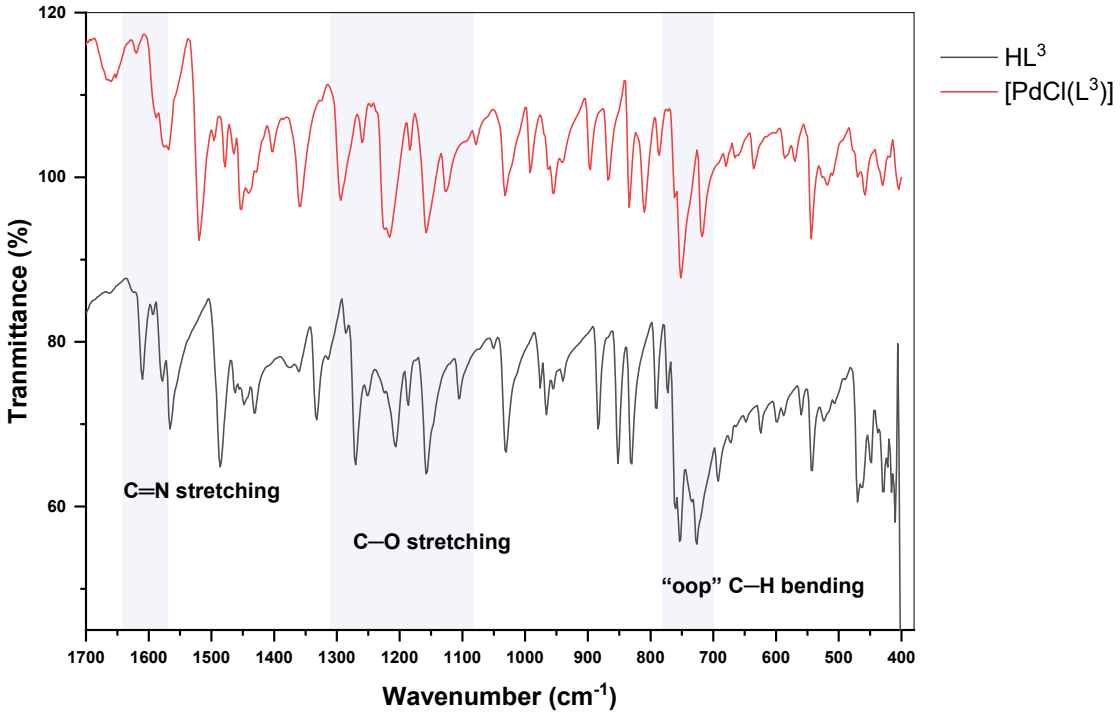

Fig. S12 FT-IR (ATR) spectra of ligand HL^3 and Pd(II) complex **3**.

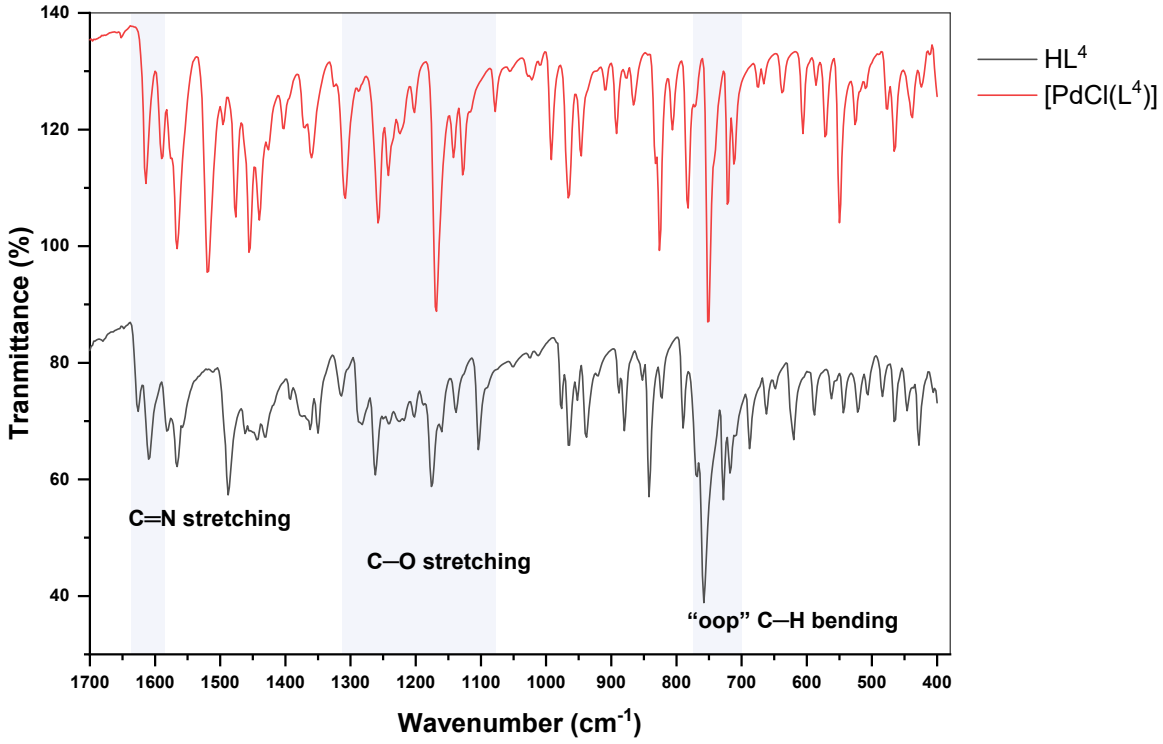

Fig. S13 FT-IR (ATR) spectra of ligand HL^4 and Pd(II) complex **4**.

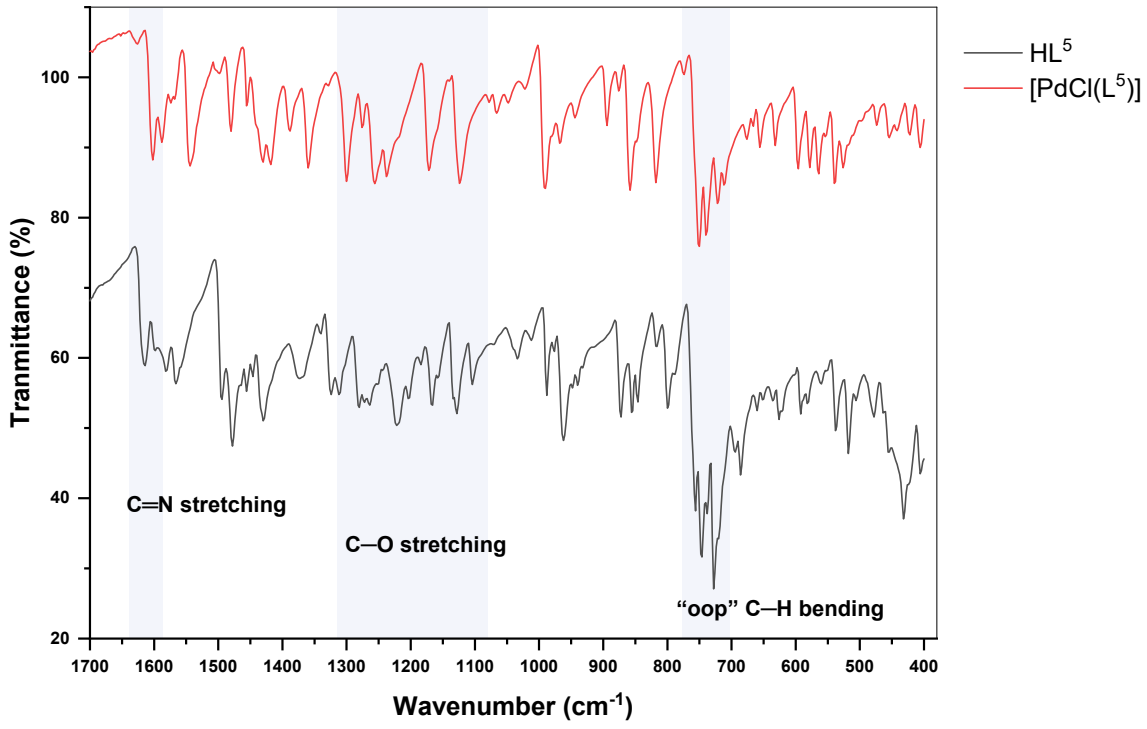

Fig. S14 FT-IR (ATR) spectra of ligand HL^5 and Pd(II) complex **5**.

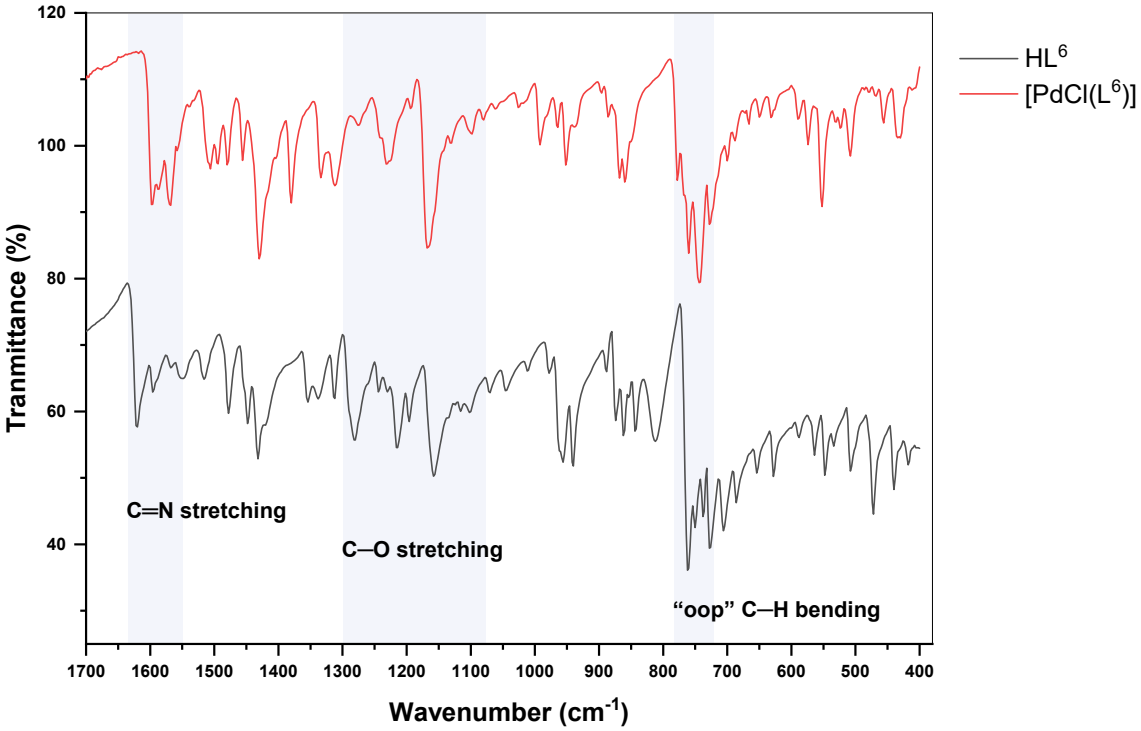

Fig. S15 FT-IR (ATR) spectra of ligand HL^6 and Pd(II) complex **6**.

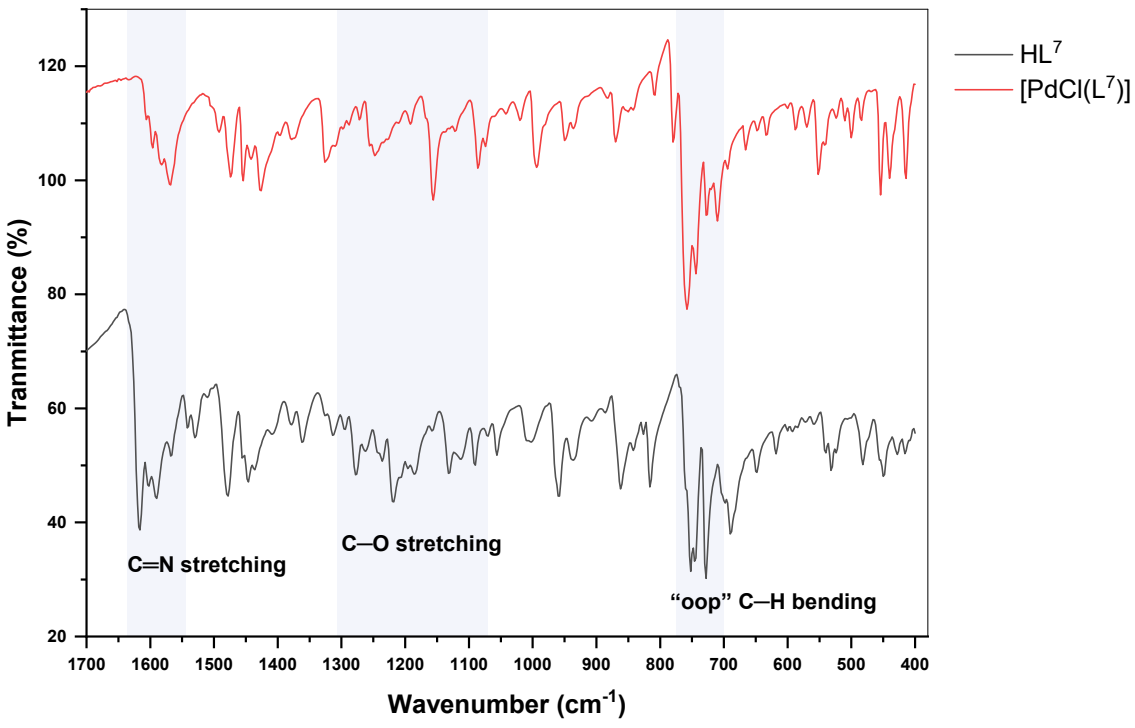

Fig. S16 FT-IR (ATR) spectra of ligand HL^7 and Pd(II) complex **7**.

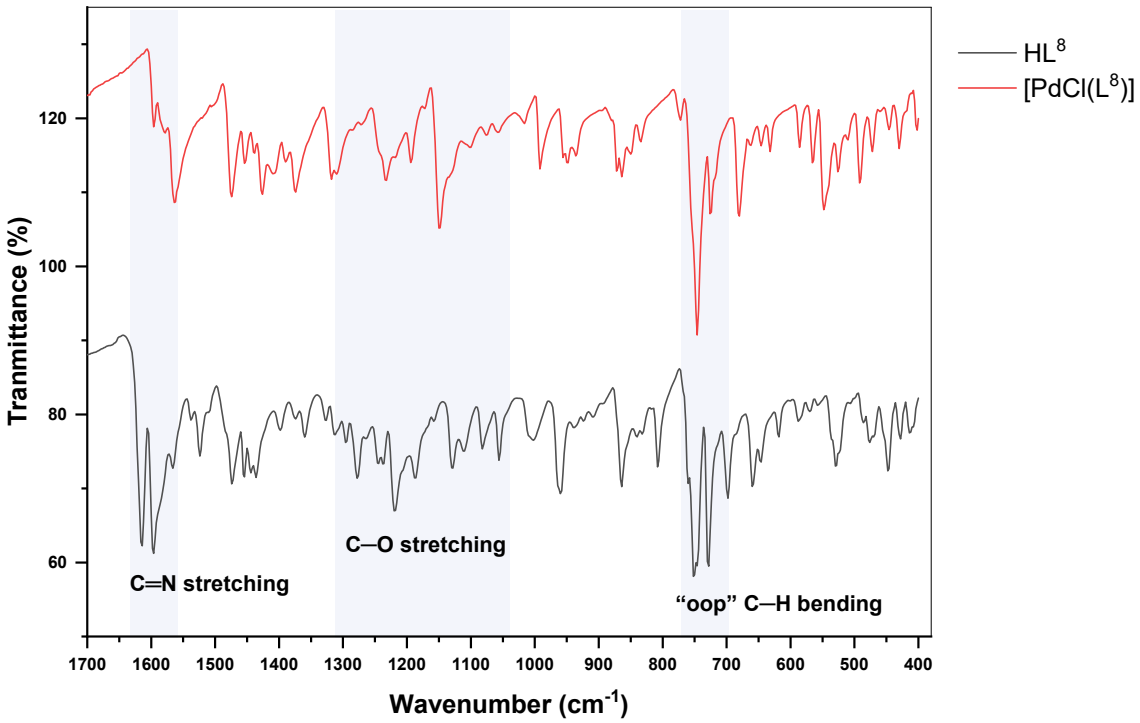

Fig. S17 FT-IR (ATR) spectra of ligand HL^8 and Pd(II) complex **8**.

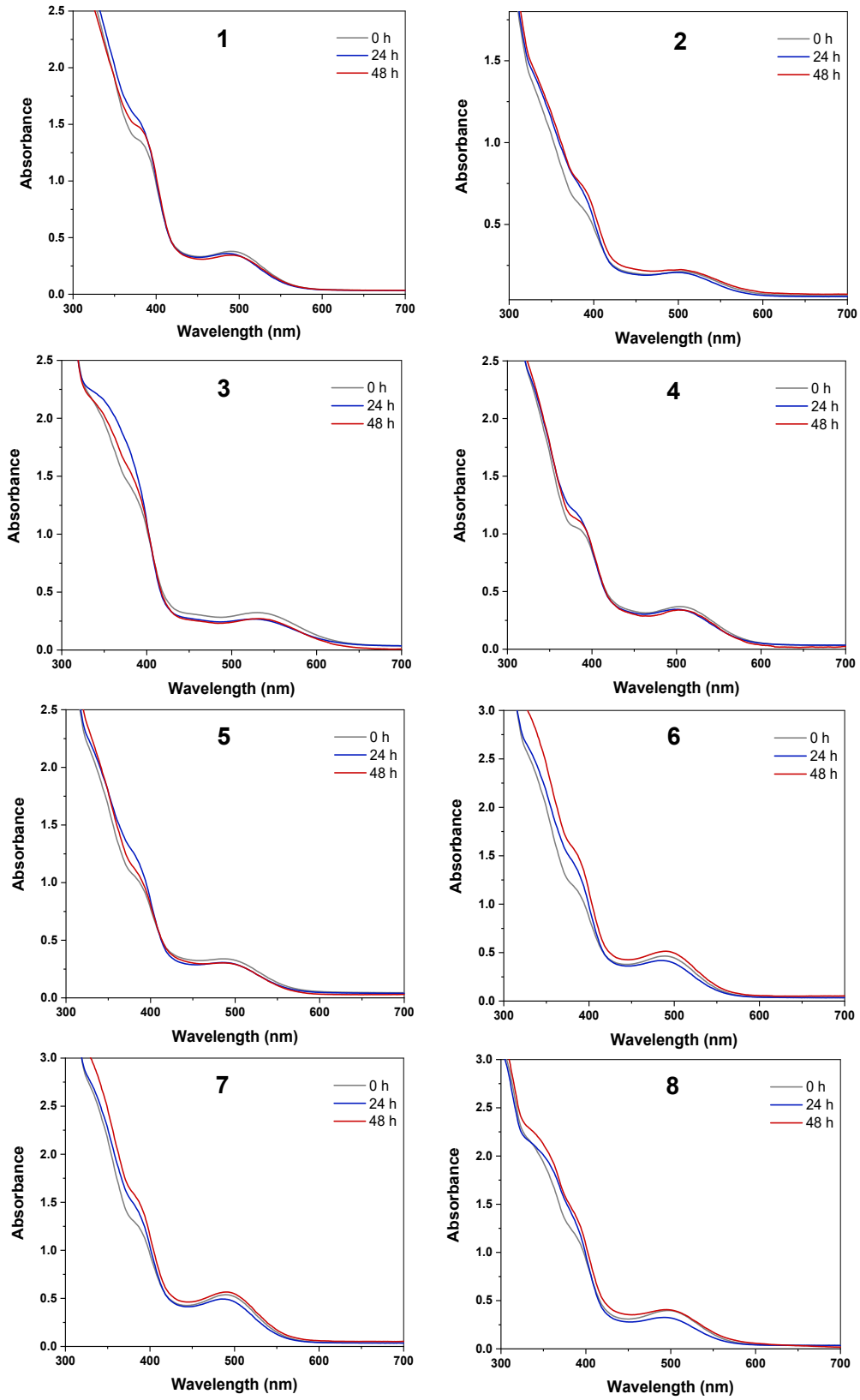

Fig. S18 UV−visible spectra of Pd(II) complexes **1**−**8** in DMSO at 25°C for 0−48 h.

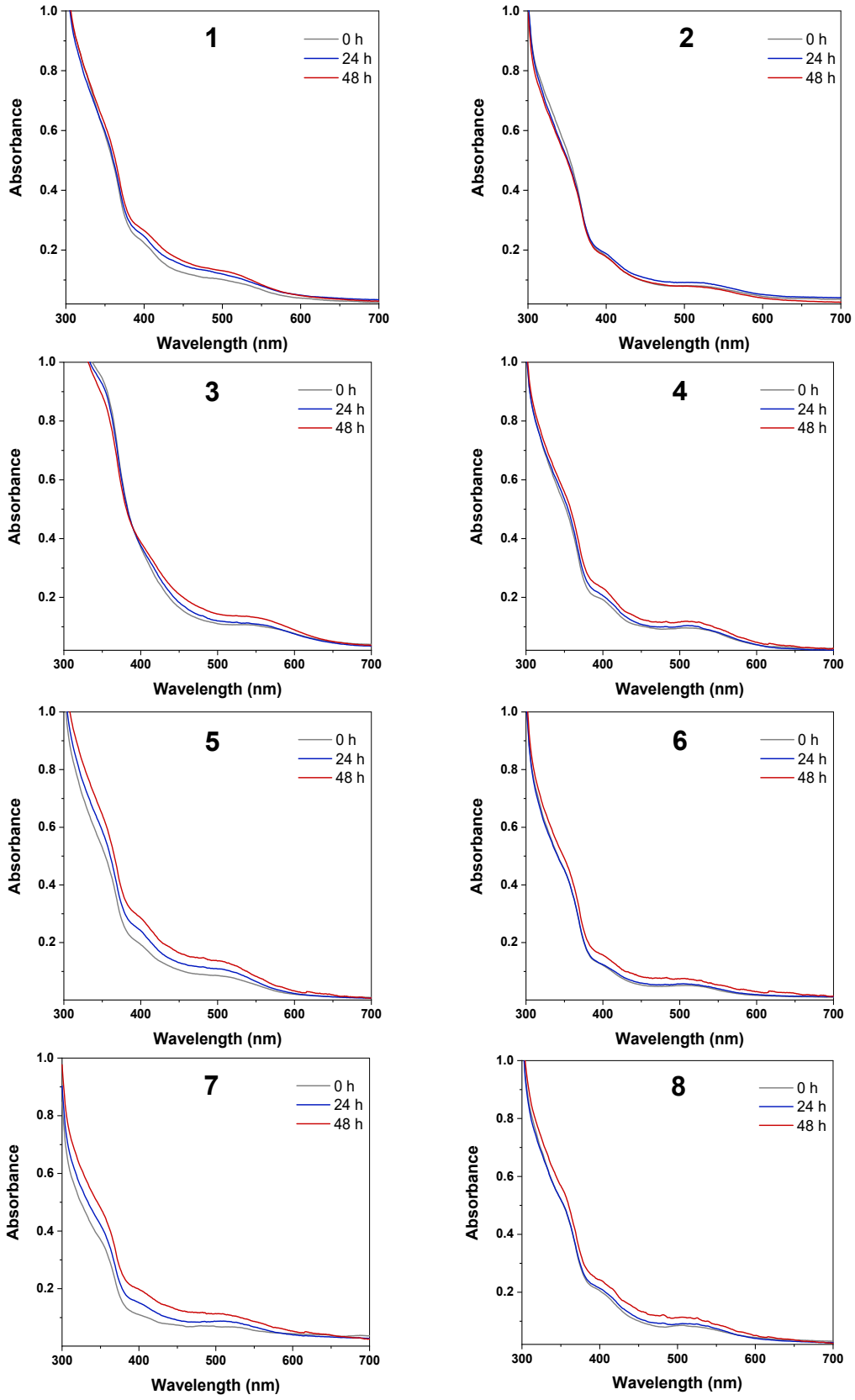

Fig. S19 UV−visible spectra of Pd(II) complexes **1**−**8** in PBS solution (pH 7.4) at 37°C for 0−48 h.

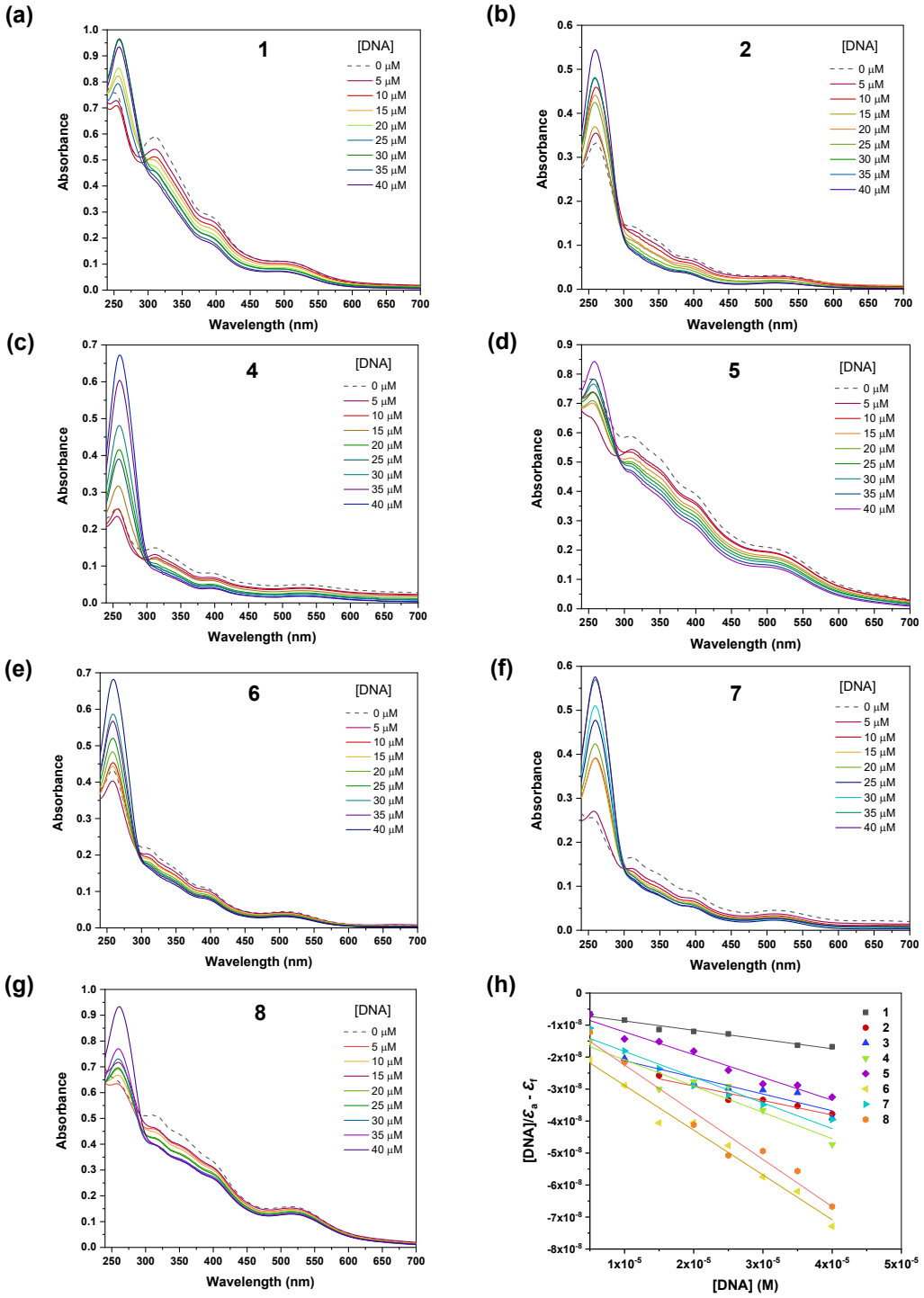

Fig. S20 UV−visible spectra of Pd(II) complexes (50 μM) in the absence and presence of CT−DNA (0−40 μM) (a−g). Wolfe−Shimer plot of [DNA] vs. [DNA]/(ε_a−ε_f) for determination of the binding constant (K_b) for Pd(II) complexes **1**−**8** (h).

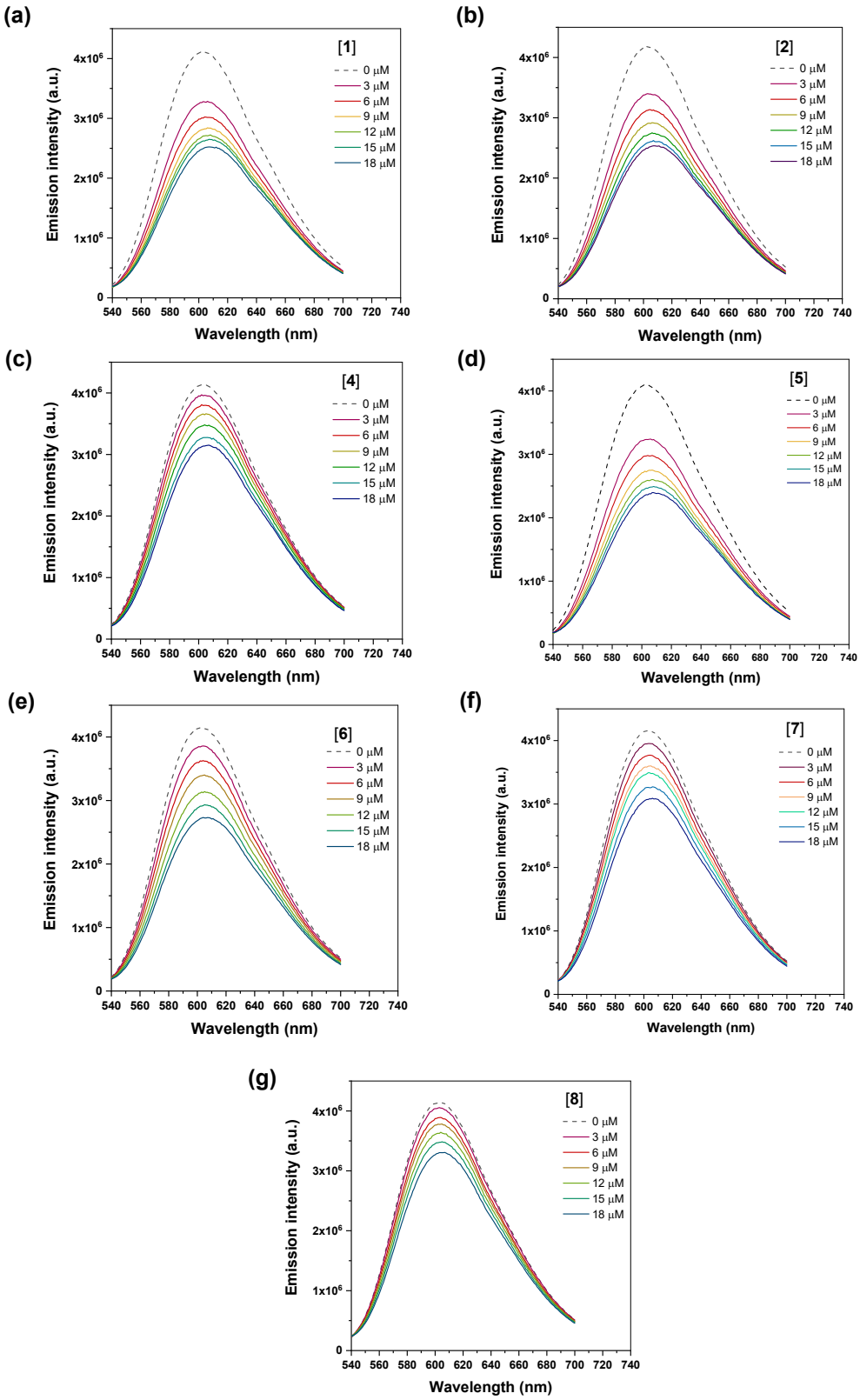

Fig. S21 Fluorescence quenching spectra of EB−DNA ([DNA] = 10 μM; [EB] = 4 μM; λ_{ex} = 525 nm; λ_{em} = 603 nm) in the absence and presence of Pd(II) complexes (0−18 μM) (a−g).

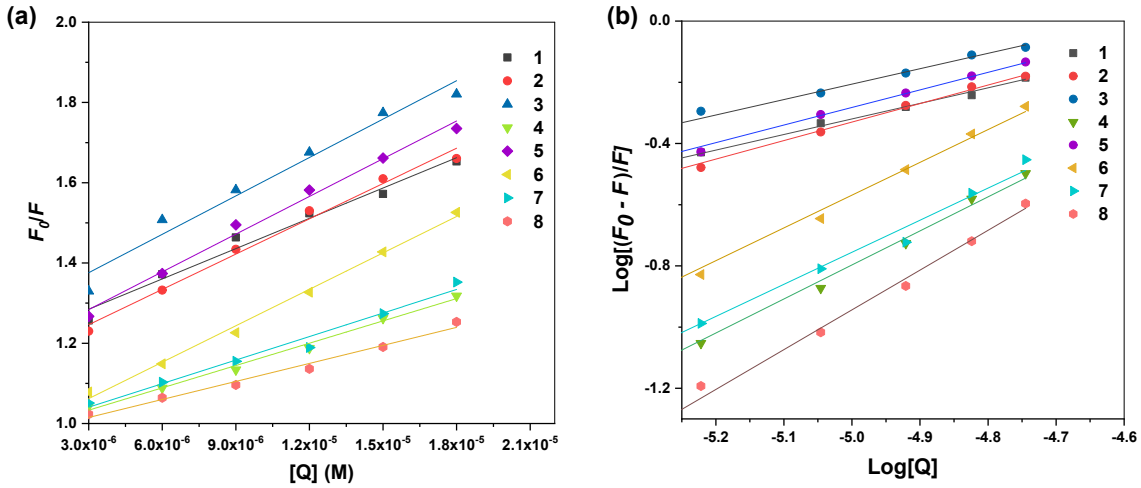

Fig. S22 Fluorescence quenching profile by **1**−**8**; Stern−Volmer plots of EB−DNA (a), and Scatchard plot of EB−DNA (b).

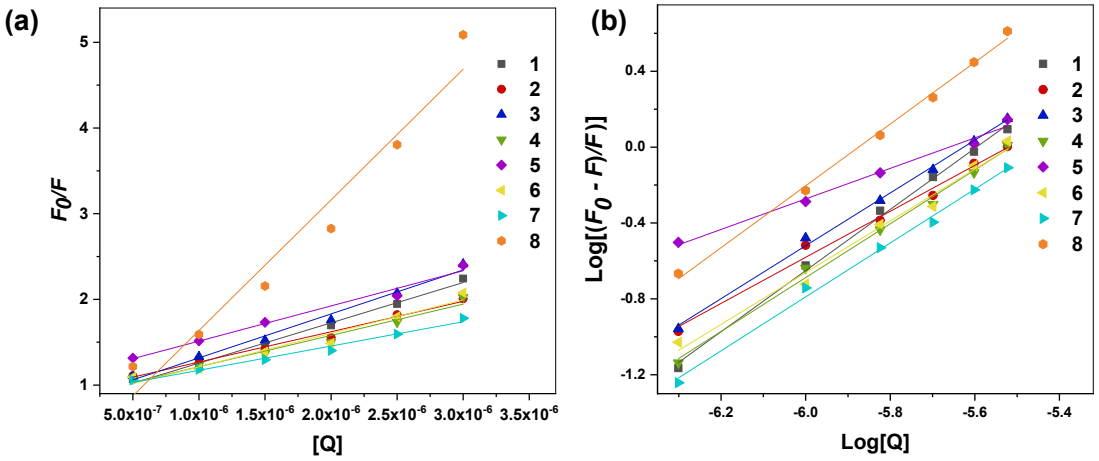

Fig. S23 Fluorescence quenching profile by complexes **1**−**8**; Stern−Volmer plots of BSA (a), and Scatchard plot of BSA (b).

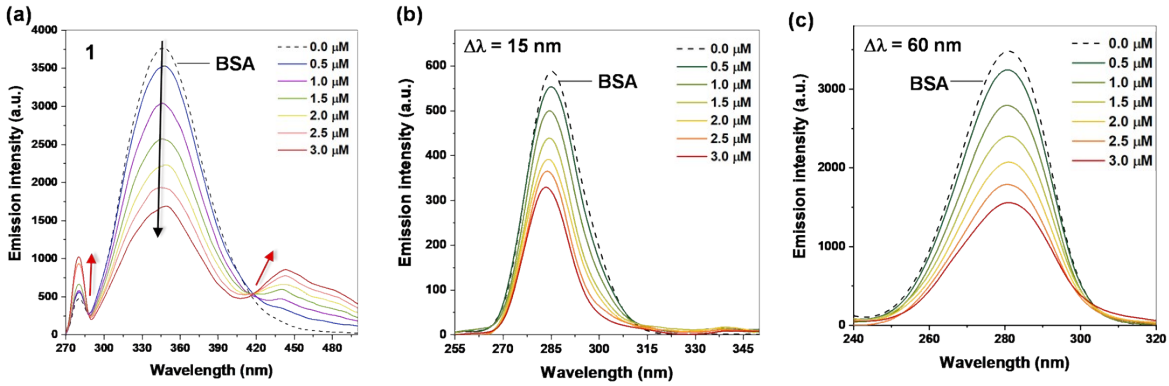

Fig. S24 Fluorescence quenching spectra of BSA (2 μM; λ_{ex} = 280 nm; λ_{em} = 350 nm) in the absence and presence of complex **1** (0−3 μM) (a). Synchronous spectra of BSA (2 μM) in the presence of increasing concentrations of complex **1** (0−3 μM) with a wavelength separation of $\Delta\lambda$ = 15 nm (b) and $\Delta\lambda$ = 60 nm (c).

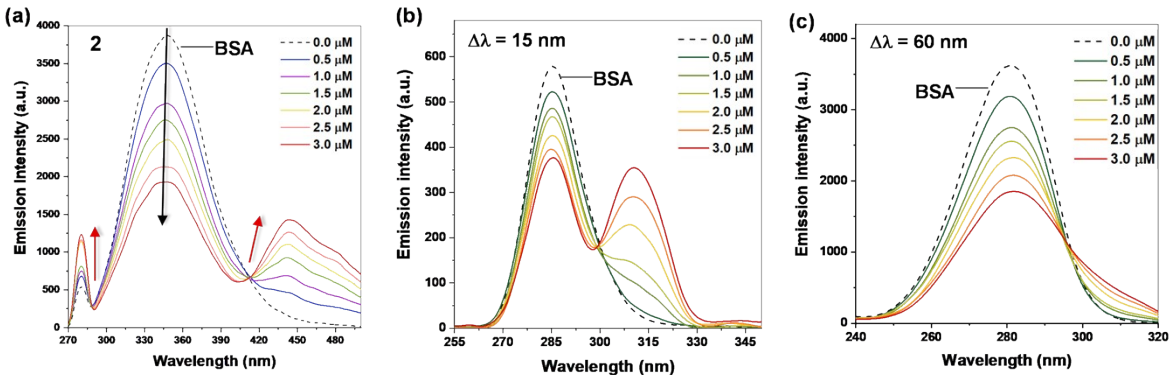

Fig. S25 Fluorescence quenching spectra of BSA (2 μM; λ_{ex} = 280 nm; λ_{em} = 350 nm) in the absence and presence of complex **2** (0−3 μM) (a). Synchronous spectra of BSA (2 μM) in the presence of increasing concentrations of complex **2** (0−3 μM) with a wavelength separation of $\Delta\lambda$ = 15 nm (b) and $\Delta\lambda$ = 60 nm (c).

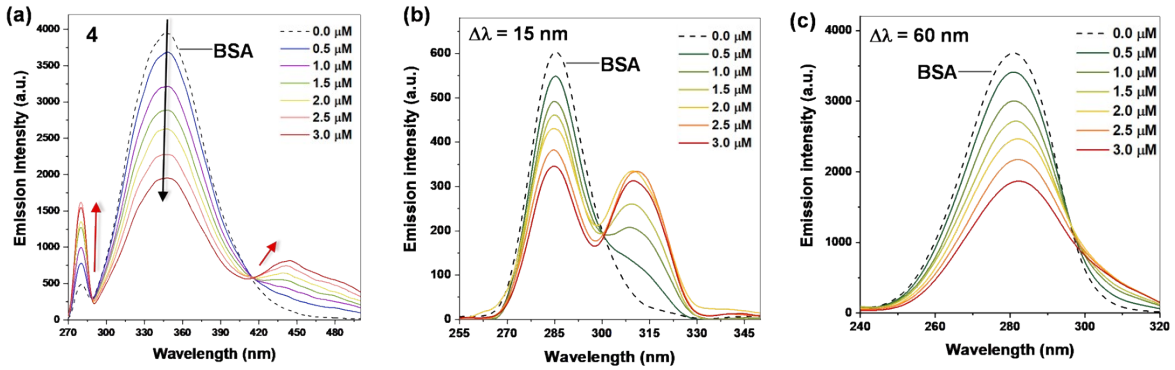

Fig. S26 Fluorescence quenching spectra of BSA (2 μM; λ_{ex} = 280 nm; λ_{em} = 350 nm) in the absence and presence of complex **4** (0−3 μM) (a). Synchronous spectra of BSA (2 μM) in the presence of increasing concentrations of complex **4** (0−3 μM) with a wavelength separation of $\Delta\lambda$ = 15 nm (b) and $\Delta\lambda$ = 60 nm (c).

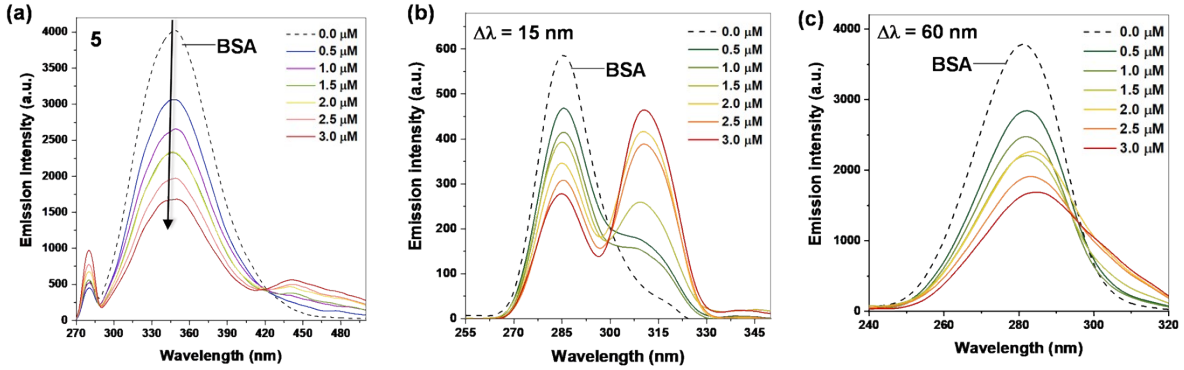

Fig. S27 Fluorescence quenching spectra of BSA (2 μM; λ_{ex} = 280 nm; λ_{em} = 350 nm) in the absence and presence of complex **5** (0−3 μM) (a). Synchronous spectra of BSA (2 μM) in the presence of increasing concentrations of complex **5** (0−3 μM) with a wavelength separation of $\Delta\lambda$ = 15 nm (b) and $\Delta\lambda$ = 60 nm (c).

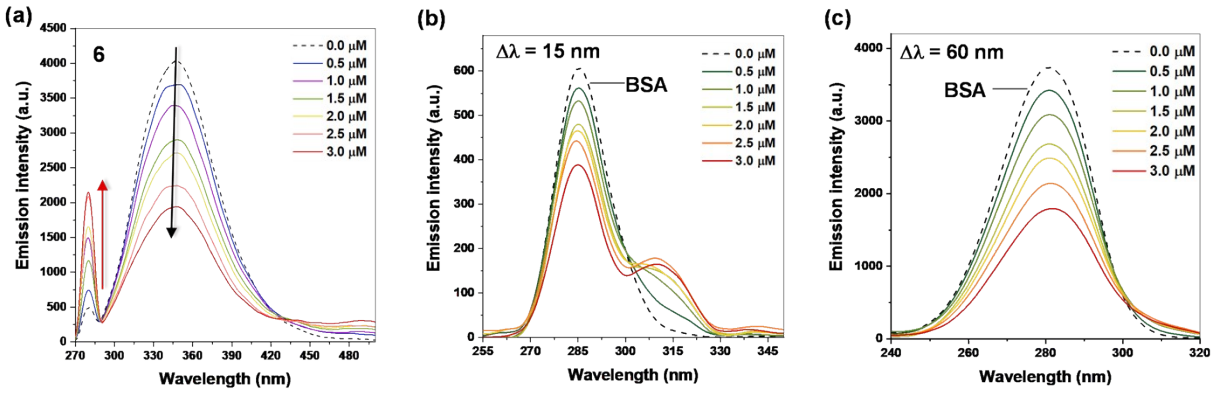

Fig. S28 Fluorescence quenching spectra of BSA (2 μM; λ_{ex} = 280 nm; λ_{em} = 350 nm) in the absence and presence of complex **6** (0−3 μM) (a). Synchronous spectra of BSA (2 μM) in the presence of increasing concentrations of complex **6** (0−3 μM) with a wavelength separation of $\Delta\lambda$ = 15 nm (b) and $\Delta\lambda$ = 60 nm (c).

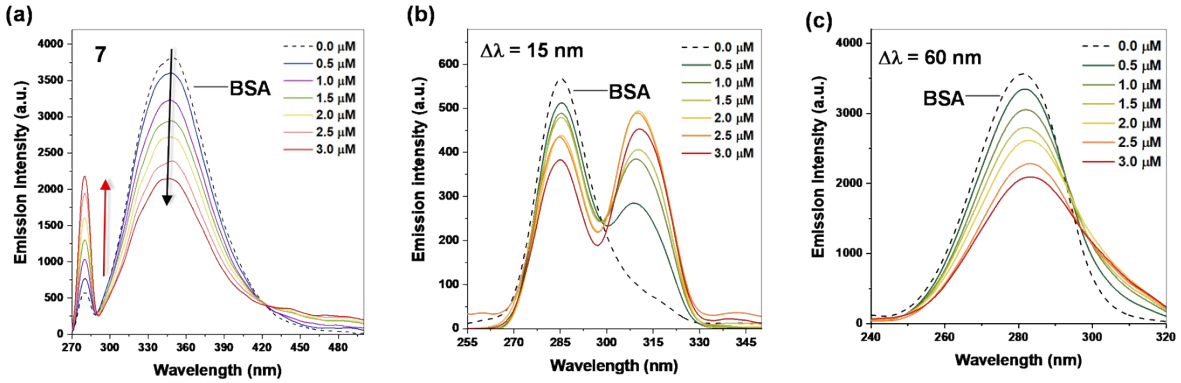

Fig. S29 Fluorescence quenching spectra of BSA (2 μM; λ_{ex} = 280 nm; λ_{em} = 350 nm) in the absence and presence of complex **7** (0−3 μM) (a). Synchronous spectra of BSA (2 μM) in the presence of increasing concentrations of complex **7** (0−3 μM) with a wavelength separation of $\Delta\lambda$ = 15 nm (b) and $\Delta\lambda$ = 60 nm (c).

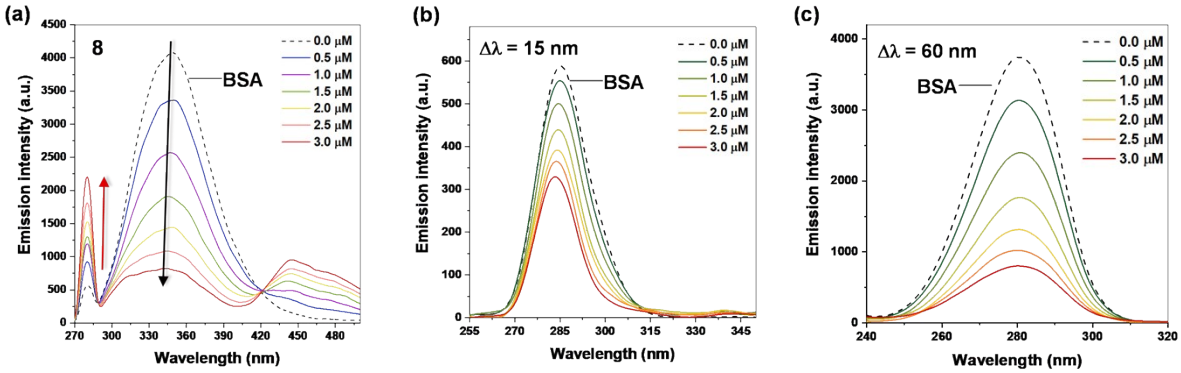

Fig. S30 Fluorescence quenching spectra of BSA (2 μM; λ_{ex} = 280 nm; λ_{em} = 350 nm) in the absence and presence of complex **8** (0−3 μM) (a). Synchronous spectra of BSA (2 μM) in the presence of increasing concentrations of complex **8** (0−3 μM) with a wavelength separation of $\Delta\lambda$ = 15 nm (b) and $\Delta\lambda$ = 60 nm (c).

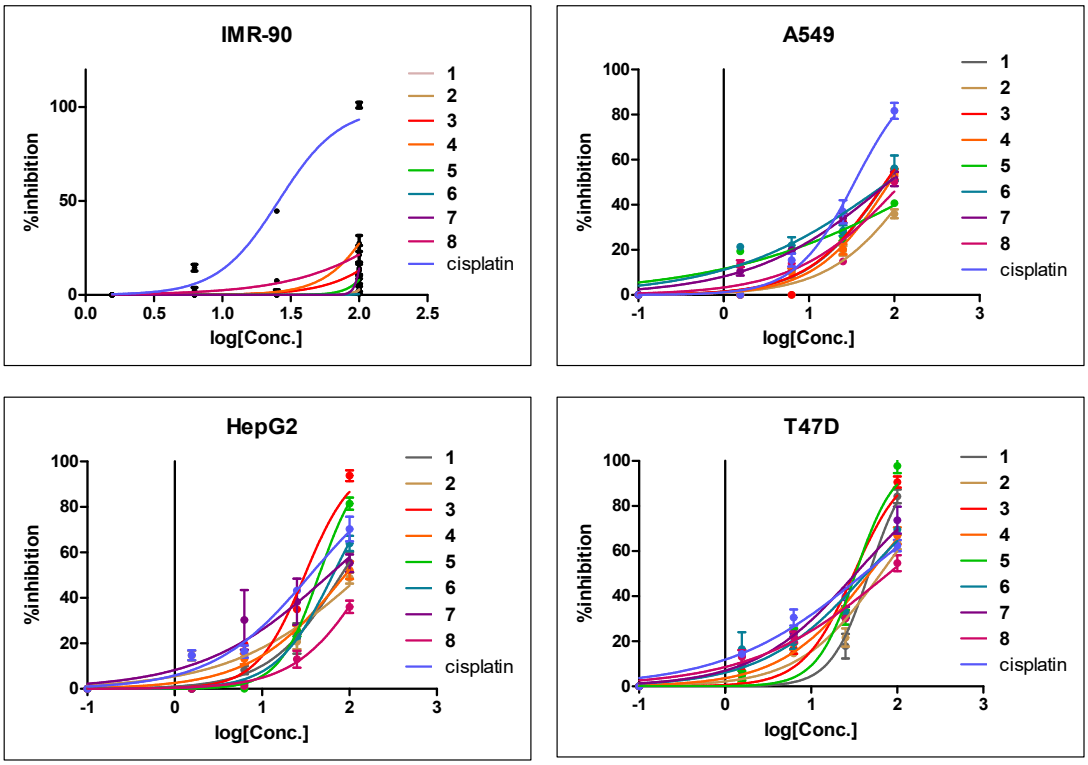

Fig. S31 Cytotoxicity of Pd(II) complexes **1**−**8** and cisplatin toward IMR−90, A549, HepG2, and T47D cell lines. IC_{50} values were fitted from the plot between %inhibition and log[concentration] using the GraphPad Prism5 software.

Table S1 Crystallographic data and structure refinement parameters for HL^2, HL^3, **1**–**3**, and **5**

	HL^2	HL^3	**1**	**2**	**3**	**5**
Empirical formula	$C_{21}H_{17}N_2OS$	$C_{21}H_{16}N_2O_2S$	$C_{20}H_{13}ClN_2OPdS$	$C_{21}H_{15}ClN_2OPdS$	$2(C_{21}H_{15}ClN_2O_2PdS)$	$C_{20}H_{11}ClF_2N_2OPdS$
Formula weight	345.42	360.44	471.27	485.30	1002.60	507.22
Temperature (K)	296.15	296.15	296.15	296.15	296.15	296.15
Crystal system	Monoclinic	Monoclinic	Monoclinic	Orthorhombic	Orthorhombic	Orthorhombic
Space group	$P2_1/c$	$P2_1/c$	$P2_1/c$	*Pbca*	*Pbca*	*Pbca*
a (Å)	10.9409(3)	10.779(4)	10.5645(13)	13.0960(10)	12.996(2)	12.4974(3)
b (Å)	12.9321(3)	12.613(4)	17.130(3)	10.9779(9)	10.9433(15)	11.1274(3)
c (Å)	13.1159(4)	13.596(4)	10.1453(14)	25.673(2)	26.809(4)	25.9429(8)
α (º)	90	90	90	90	90	90
β (º)	111.9350(10)	110.290(13)	105.873(5)	90	90	90
γ (º)	90	90	90	90	90	90
V (Å^3)	1721.41(8)	1733.8(10)	1766.0(4)	3691.0(5)	3812.9(10)	3607.71(17)
Z	4	4	4	8	4	8
F(000)	720.7704	752.8144	933.4216	1930.8628	1994.9499	2000

D_c (g cm^{-3})	1.3289	1.3807	1.7724	1.7465	1.7464	1.868
μ (mm^{-1})	0.199	0.205	1.332	1.277	1.243	1.326
θ range (°)	2.61 to 28.35	2.58 to 28.32	3.11 to 28.33	2.55 to 26.41	3.13 to 30.59	2.91 to 28.34
Reflections collected	43327	61709	49008	63511	105897	153380
Max., min transmission	0.7457, 0.6566	0.7457, 0.6870	0.7457, 0.6926	0.7454, 0.6209	0.7461, 0.6835	0.7457, 0.6664
$R_{(int)}$	0.0842	0.0509	0.0491	0.0759	0.0450	0.0516
Goodness−of−fit on F^2	1.0574	1.0695	1.0624	1.0393	1.0459	1.154
Final R indexes [I>=2σ (I)]: R_1, wR_2	0.0432, 0.0979	0.0385, 0.0955	0.0265, 0.0644	0.0672, 0.1678	0.0368, 0.0718	0.0299 ,0.0619
Final R indexes [all data]: R_1, wR_2	0.0810, 0.1185	0.0502, 0.1035	0.0342, 0.0693	0.0729, 0.1711	0.0438, 0.0749	0.0357, 0.0643
Largest diff. peak/hole (e Å^{-3})	0.2512/−0.3004	0.2660/−0.3385	0.7172/−0.6565	1.4601/−2.0156	0.7130/−0.9514	0.374/−0.589
CCDC no.	2068395	2068691	2216314	2216316	2216315	2216317

Table S2 Selected bond lengths (Å), bond angles (˚), and dihedral angles (˚) for HL^2.

Bond lengths		Bond angles		Dihedral angles	
N1–C1	1.296(3)	N1–C1–C8	120.8(2)	C2–N1–C1–C8	−176.6(2)
N1–C2	1.386(3)	N2–C9–C8	119.9(2)	N2–C9–C8–C1	5.0(3)
N2–C9	1.419(2)	N2–C14–C15	123.4(2)	C9–N2–C14–C15	−174.9(2)
N2–C14	1.282(2)	C9–N2–C14	118.6(2)	N2–C14–C15–C16	6.7(3)
S1–C1	1.749(2)	C15–C16–O1	121.7(2)	C14–C15–C16–O1	−0.7(3)
O1–C16	1.360(3)	S1–C1–C8	124.0(1)	C9–C8–C1–S1	12.4(3)

Table S3 Selected bond lengths (Å), bond angles (˚), and dihedral angles (˚) for HL^3.

Bond lengths		Bond angles		Dihedral angles	
N1–C6	1.381(2)	N1–C7–C8	121.5(1)	C6–N1–C7–C8	−177.9(1)
N1–C7	1.298(2)	N2–C13–C8	119.9(1)	N2–C13–C8–C7	2.6(2)
N2–C13	1.415(2)	N2–C14–C15	122.8(1)	C13–N2–C14–C15	−175.9(1)
N2–C14	1.283(2)	C13–N2–C14	118.3(1)	N2–C14–C15–C16	6.9(2)
S1–C7	1.754(1)	C15–C16–O1	122.3(1)	C14–C15–C16–O1	−1.2(2)
O1–C16	1.359(2)	S1–C7–C8	123.7(1)	C13–C8–C7–S1	10.1(2)

Table S4 Selected bond lengths (Å), bond angles (˚), and dihedral angles (˚) for complex **1**.

Bond lengths		Bond angles		Dihedral angles	
N1–C7	1.299(3)	N1–C7–C6	125.9(2)	C15–N2–C14–C13	−173.2(3)
N1–C8	1.423(4)	N1–C8–C13	121.1(3)	N1–C8–C13–C14	−4.6(5)
N2–C14	1.312(4)	N2–C14–C13	125.9(3)	C8–N1–C7–C6	165.1(2)
N2–C15	1.406(3)	C8–N1–C7	118.8(2)	N1–C7–C6–C1	−17.4(4)
S1–C14	1.726(3)	C6–C1–O1	124.9(2)	C7–C6–C1–O1	7.7(4)

O1–C1	1.312(3)	S1–C14–C13	119.6(2)	C8–C13–C14–S1	−150.3(3)
Pd1–N1	1.994(2)	N1–Pd1–N2	88.55(8)	O1–Pd1–N1–C8	−144.2(2)
Pd1–N2	2.027(2)	N2–Pd1–Cl1	95.38(6)	N2–Pd1–O1–C1	48.4(5)
Pd1–O1	1.981(2)	O1–Pd1–Cl1	87.74(6)	N2–Pd1–N1–C7	−139.2(2)
Pd1–Cl	2.3286(8)	O1–Pd1–N1	90.63(8)	N2–Pd1–N1–C8	47.1(2)

Table S5 Selected bond lengths (Å), bond angles (˚), and dihedral angles (˚) for complex **2**.

Bond lengths		Bond angles		Dihedral angles	
N1–C1	1.40(1)	N1–C7–C8	125.6(7)	C1–N1–C7–C8	174.5(7)
N1–C7	1.30(1)	N2–C13–C8	122.1(7)	N2–C13–C8–C7	−4(1)
N2–C13	1.412(9)	N2–C14–C15	126.3(7)	C13–N2–C14–C15	−166.0(7)
N2–C14	1.305(9)	C13–N2–C14	119.0(6)	N2–C14–C15–C20	36.0(5)
S1–C7	1.741(8)	C15–C20–O1	123.3(6)	C14–C15–C20–O1	−6(1)
O1–C20	1.311(9)	S1–C7–C8	119.7(6)	C13–C8–C7–S1	156.9(7)
Pd1–N1	2.029(7)	N1–Pd1–N2	88.2(3)	O1–Pd1–N2–C13	145.8(5)
Pd1–N2	1.994(6)	N1–Pd1–Cl1	95.3(2)	N1–Pd1–O1–C20	− 50(1)
Pd1–O1	1.973(5)	O1–Pd1–Cl1	88.3(2)	N1–Pd1–N2–C13	−46.8(5)
Pd1–Cl	2.331(2)	O1–Pd1–N2	91.0(2)	N1–Pd1–N2–C14	141.6(6)

Table S6 Selected bond lengths (Å), bond angles (˚), and dihedral angles (˚) for complex **3**.

Bond lengths		Bond angles		Dihedral angles	
N1–C1	1.405(4)	N1–C7–C8	126.2(2)	C1–N1–C7–C8	175.6(3)
N1–C7	1.308(3)	N2–C13–C8	120.6(2)	N2–C13–C8–C7	−3.5(4)
N2–C13	1.420(3)	N2–C14–C15	125.4(2)	C13–N2–C14–C15	−168.8(2)
N2–C14	1.297(3)	C13–N2–C14	118.2(2)	N2–C14–C15–C20	19.8(4)

S1–C7	1.737(3)	C15–C20–O1	124.7(2)	C14–C15–C20–O1	−4.9(4)
O1–C20	1.317(3)	S1–C7–C8	119.7(2)	C13–C8–C7–S1	157.4(2)
Pd1–N1	2.035(2)	N1–Pd1–N2	88.57(9)	O1–Pd1–N2–C13	145.1(2)
Pd1–N2	1.985(2)	N1–Pd1–Cl1	95.26(7)	N1–Pd1–O1–C20	−45.1(5)
Pd1–O1	1.984(2)	O1–Pd1–Cl1	88.61(6)	N1–Pd1–N2–C13	−47.4(2)
Pd1–Cl	2.3322(7)	O1–Pd1–N2	90.37(8)	N1–Pd1–N2–C14	139.4(2)

Table S7 Selected bond lengths (Å), bond angles (˚), and dihedral angles (˚) for complex **5**.

Bond lengths		Bond angles		Dihedral angles	
N1–C1	1.401(3)	N1–C7–C8	125.7(2)	C1–N1–C7–C8	−174.6(2)
N1–C7	1.311(3)	N2–C13–C8	121.1(2)	N2–C13–C8–C7	2.1(4)
N2–C13	1.428(3)	N2–C14–C15	125.4(2)	C13–N2–C14–C15	166.6(2)
N2–C14	1.288(3)	C13–N2–C14	118.8(2)	N2–C14–C15–C16	−17.6(4)
S1–C7	1.729(2)	C15–C16–O1	126.6(2)	C14–C15–C16–O1	4.6(4)
O1–C16	1.304(3)	S1–C7–C8	120.1(2)	C13–C8–C7–S1	−155.6(2)
Pd1–N1	2.029(2)	N1–Pd1–N2	87.81(8)	O1–Pd1–N2–C13	−143.7(3)
Pd1–N2	1.984(2)	N1–Pd1–Cl1	94.76(6)	N1–Pd1–O1–C16	39.8(4)
Pd1–O1	1.997(2)	O1–Pd1–Cl1	89.87(5)	N1–Pd1–N2–C13	48.4(2)
Pd1–Cl	2.3263(7)	O1–Pd1–N2	90.13(8)	N1–Pd1–N2–C14	−136.8(2)

Table S8 Free energy of binding of the complexes with biomolecules.

Complex	Free energy of binding (kcal mol^{-1})[a]		
	DNA (PDB ID: 1BNA)	DNA (PDB ID: 1Z3F)	BSA (PDB ID: 4F5S)
3	−9.07	−8.49	−9.40
5	−7.79	−7.38	−7.97

[a]Best complex pose according to Autodock

Table S9 Active site residues of DNA and BSA involved in non-bonded interactions with the complexes.

Complex	Active site residues		
	DNA (PDB ID: 1BNA)	DNA (PDB ID: 1Z3F)	BSA (PDB ID: 4F5S)
3	DT8, DT19, DT20	DG2, DC1, DC5, DG6	Pro117, Leu115, Lys144, Ile181, Arg185, Arg144, His185
5	DT7, DC9, DA18, DT19, DT20	DG2, DC1, DC5, DG6, DA3	Pro110, Asp108, Arg458, Glu424, His145, Arg193, Arg196

Ligand	A549	HepG−2	T47D	IMR−90	SI[b]		
					A549	HepG−2	T47D
HL[1]	>100	>100	>100	>100	~1	~1	~1
HL[2]	>100	68.6 ± 7.6	>100	>100	~1	1.46	~1
HL[3]	>100	87.3 ± 13.5	76.8 ± 6.0	>100	~1	1.15	1.30
HL[4]	>100	46.3 ± 4.1	>100	>100	~1	2.16	~1
HL[5]	>100	>100	51.9 ± 1.8	>100	~1	~1	1.93
HL[6]	>100	44.9 ± 6.4	38.7 ± 0.5	>100	~1	2.23	2.58
HL[7]	>100	50.3 ± 3.4	32.2 ± 10.8	>100	~1	1.99	3.10
HL[8]	>100	47.2 ± 0.9	46.2 ± 21.6	>100	~1	2.19	2.16

Table S10 IC_{50} values in different human cancer and normal cell lines (48 h) of Schiff base ligands.